

Superconducting NbN-Nanowire Single-Photon Detectors Capable of Photon Number Resolving

A. Korneev, A. Divochiy, M. Tarkhov, O. Minaeva, V. Seleznev, N. Kaurova,
B. Voronov, O. Okunev, G. Chulkova, I. Milostnaya, K. Smirnov and G. Gol'tsman

Moscow State Pedagogical University, Moscow 119992, Russia

E-mail: akorneev@rplab.ru

Abstract - We present our latest generation of ultra-fast superconducting NbN single-photon detectors (SSPD) capable of photon-number resolving (PNR). The novel SSPDs combine $10\ \mu\text{m} \times 10\ \mu\text{m}$ active area with low kinetic inductance and PNR capability. That resulted in significantly reduced photoresponse pulse duration, allowing for GHz counting rates. The detector's response magnitude is directly proportional to the number of incident photons, which makes this feature easy to use. We present experimental data on the performance of the PNR SSPDs. These detectors are perfectly suited for fibreless free-space telecommunications, as well as for ultra-fast quantum cryptography and quantum computing.

Received December 14, 2007; accepted March 14, 2008. Reference No. ST34; Category 4.
Paper accepted for Proceedings of EUCAS 2007; published in JPCS **98** (2008), paper # 012307

I. INTRODUCTION

Novel photonics experiments and applications rely on ultra-fast, robust and efficient single-photon detectors capable of photon number resolving (PNR). Quantum communication and quantum computing use multi-photon states with low (1 to 5) number of photons for establishing, transfer and measuring of entanglement. This is presently realised by correlating the output of several detectors, a technique which is resource-intensive and not scalable to large photon numbers. In the quantum key distribution systems based on heavily attenuated laser pulses the secure distance can be significantly enlarged when protocols based on multi-photon states are used. This allows one to detect photon-number-splitting attacks based on the measured photon statistics and avoid the usage of truly single-photon sources. In the traditional 10 Gb/s optical communication the use of photon number resolving techniques will reduce the minimum sensitivity threshold to the level of tens of photons and enlarge the un-amplified link distance. Until present, it was impossible to replace the avalanche photodiodes (APDs) with single-photon detectors in the optical link due to impossibility of distinguishing reliably "on" and "off" states of the light source – a consequence of peculiarities of its modulation. In fluorescence spectroscopy, PNR detectors could replace time-correlated single-photon counting by providing a direct optical-to-electrical linear conversion and thus the possibility of measuring the temporal decay of a weak fluorescence signal in real time. This would improve the speed and sensitivity of single-molecule fluorescence instrumentation for biological and pharmaceutical applications. PNR detectors make possible the direct measurement of the photon statistics of the luminescence from single molecules and quantum

dots. Optical time domain reflectometry (OTDR) will also gain in speed and sensitivity if a fast and reliable photon-number detector is used.

It was recently demonstrated that the NbN nanowire superconducting single-photon detector (SSPD) [1, 2] has a performance similar or better than its nearest competitors: semiconductor single-photon avalanche photodiodes (APD), photomultiplier tubes (PMT) as well as superconducting transition edge sensors (TES). The SSPD is patterned from 4-nm-thick NbN film as a meander-shaped stripe which covers a square area of $10\ \mu\text{m} \times 10\ \mu\text{m}$. The stripe is 120-nm-wide and the gap between the neighboring stripes of the meander is 80 nm which provides the 60% filling factor (the ratio of the area covered by the superconducting film to the whole area of $10\ \mu\text{m} \times 10\ \mu\text{m}$). The SSPD is operated well below its critical temperature T_c (typically at 2-3 K whereas T_c is ~ 10 K) and biased by a current close to the critical current. The operation principle is based on the formation of a resistive region in the place of photon absorption (so called "hot spot") with the subsequent redistribution of the bias current around the hot spot. When the current density in the "sidewalks" around the hotspot exceeds the critical current density the entire cross-section of the stripe becomes resistive which manifests itself as a voltage pulse on the terminals of the SSPD [3].

We demonstrated that the SSPD has a quantum efficiency η (the ratio of the detection events to the number of photons falling on the SSPD) in the near infrared (1.5- μm wavelength) close to 30% [4]. This is limited by NbN film absorption. It was also independently demonstrated in [5] and [6] that η can reach $\sim 60\%$ by implementing a microcavity resonator [6]. The η drops with the wavelength increase and remains reasonably high ($\sim 0.4\%$) at 5.6 μm wavelength making SSPDs the only practical detector in mid-infrared [7]. The dark counts rate R_{dk} drops exponentially with the bias current decrease and can be as low as $2 \times 10^{-4}\ \text{s}^{-1}$ [4]. Another essential parameter for time-correlating research techniques is the photon detection timing accuracy (jitter) which for SSPD is below 20 ps including the jitter of the electronics [8]. The maximum counting rate of the SSPD is limited by the kinetic inductance of the superconducting stripe; it was shown by A. Kerman et al [9] that the $10 \times 10\ \mu\text{m}^2$ active area response time is in the nanosecond range.

Because of the favourable characteristics and the possibility to be effectively coupled to single-mode optical fibre [10] many applications of the SSPD are possible and have been reported. The most impressive is the report on the quantum key distribution (QKD) over 200 km distance [11]. Other QKD experiments also were reported in [12], [13] as well as the non-quantum optical communication [14]. The implementation of the SSPD for the research into emission of single-photon sources, e.g., quantum dots or quantum wells, by time-correlated single-photon counting methods were reported as well [15, 16].

Recently we reported the development of ultrafast SSPD capable of counting rates above 1 GHz. It employs the same hot-spot response mechanism, but features significantly smaller kinetic inductance, which was attained by connecting superconducting stripes in parallel [7]. This approach turned out to be also fruitful for photon number resolving. The same device combines both ultrafast (sub nanosecond) response time and photon number resolving capability. In this paper we describe our recent study of this novel SSPD with PNR capability (PNR-SSPD).

II. DESIGN OF PNR-SSPD

To realize the photon-number-resolving capability we use several superconducting strips connected in parallel. Although at first glance it may seem that the remaining superconducting

strips should shunt the resistive strip that absorbed a photon this does not actually happen. The reason is the kinetic inductance of the long and narrow superconducting strips. Figure 1 present the equivalent electrical circuits of the traditional single-strip SSPD (a) and the new photon-number resolving SSPD (b). In both circuits the resistors R_b and R_l represent the internal resistance of the bias source and of the transmission line (coaxial cable), respectively.

When the SSPD is in the superconducting state we may assume that the switch in Figure 1(a) is closed. When a photon is absorbed we may assume that the switch opens and the resistance R appears. The bias source should be a voltage source. In this case the bias current through the SSPD drops after opening of the switch, leading to the reduction of the Joule heating of the resistive region, and the superconductivity restores spontaneously.

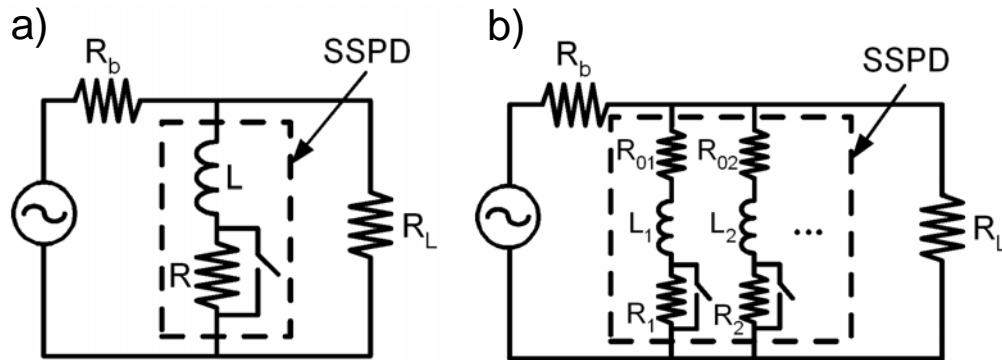


Fig. 1. Equivalent circuit of the SSPD consisting of one superconducting stripe (a) and equivalent circuit of PNR-SSPD consisting of several superconducting stripes connected in parallel (b). Resistors R_b and R_l represent the internal resistance of the bias source and of the transmission line (coaxial cable), respectively. Resistors R , R_1 , R_2 represent the resistance that appears after photon absorption. Inductances L , L_1 , L_2 represent the kinetic inductance of the superconducting strip. Resistors R_{01} , R_{02} are required to provide controllable bias current distribution between the stripes and to suppress unwanted normal state transition of the stripes that did not absorb a photon.

A similar mechanism can be observed in the "multi-strip" PNR-SSPD. Let's assume that the photon was absorbed by strip #1 of Figure 1(b). We may treat this as opening of switch #1 and appearance of the resistance R_1 . The presence of R_b makes the bias conditions similar to current-bias regime. The bias current of strip #1 drops, simultaneously bias currents of all the other strips increase.

Due to the kinetic inductance, the impedance of those stripes is comparable with the impedance of the transmission line and a certain part of the bias current flows through it providing a voltage pulse. If two stripes become resistive simultaneously the portion of the bias current expelled to the transmission line will be higher (numerical simulation shows that it should be almost twice as high as in the case of single stripe switch) providing a higher voltage pulse and permitting to distinguish the number of simultaneously detected photons by the magnitude of the response voltage.

The resistors R_{01} , R_{02} , etc., connected in series to each stripe serve two purposes: first, they make the distribution of the bias current between the strips controllable, and second, they suppress the switching of several strips upon one photon absorption. Indeed, the opening of switch #1 in the example above causes the bias currents in all the strips except #1 to increase. As the SSPD is operated close to its critical current the increasing current may exceed the critical current of any single stripe and will switch it to the resistive state too. The resulting response pulse would have higher magnitude and would be indistinguishable from two-

photon response. The resistors connected in series to each stripe reduce the current increase and allow operation closer to the critical current.

III. PNR-SSPD FABRICATION

The SSPD fabrication process is based on conventional electron beam lithography. As the SSPD is biased close to its critical current, the fabrication of very uniform long stripes with a minimum of defects is vitally important. Indeed, any weak point in the stripe will limit the critical current and reduce the quantum efficiency of the device. We developed a process that allows us to fabricate conventional SSPDs with a quantum efficiency up to 30%, which is close to its ultimate value limited by the NbN film absorption. In this process we use e-beam lithography for drawing of straight lines oriented along the x- or y- axis of the e-beam writer. The NbN film will be later removed from these lines and they will become the gaps between the stripes of the meander. The width of these lines is 80 nm and the variation of the width is less than several nanometers. The gap between the lines (the width of the NbN stripe) is 120 nm. Then, to form the meander, we remove the NbN film in the photolithography process from everywhere except the rectangular area between the gold contact pads (the NbN film remains also below the gold contact pads).

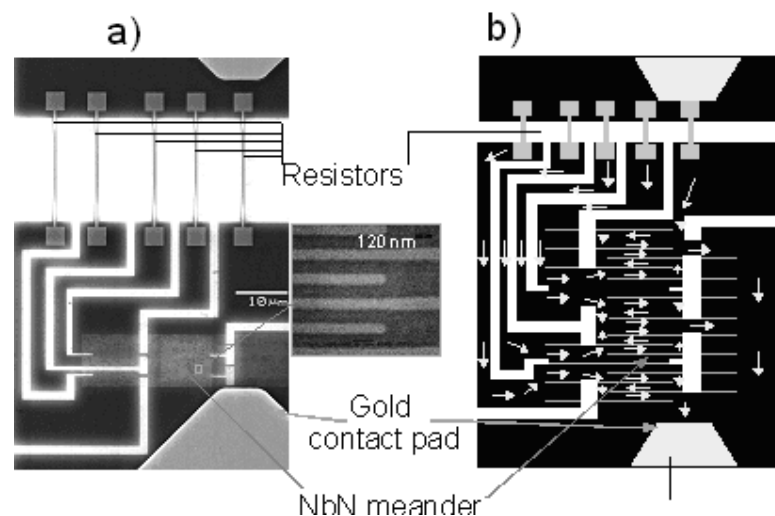


Fig. 2. (a) SEM image of the 5-section PNR-SSPD; black is the NbN film, white are the areas from which the film is removed. The drawing (b) explains how five meander-shaped strips are connected in series to planar resistors and then all the strips with their resistors are connected in parallel to the contact pads. Again, black is the NbN, white are the areas without NbN; the arrows indicate the bias current flow.

The basic idea in multi-strip PNR-SSPD fabrication is to use the already developed process of single-meander SSPD fabrication. Figure 2(a) presents the SEM image of the PNR-SSPD, the inset is taken at the edge of the meander and shows 120-nm-wide NbN stripes (black in

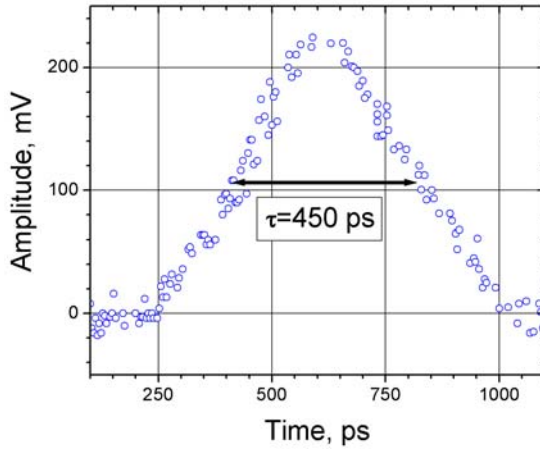


Fig. 3 Precisely acquired waveform transient of PNR SSPD response for a single photon. The full width at half of the maximum is 450 ps.

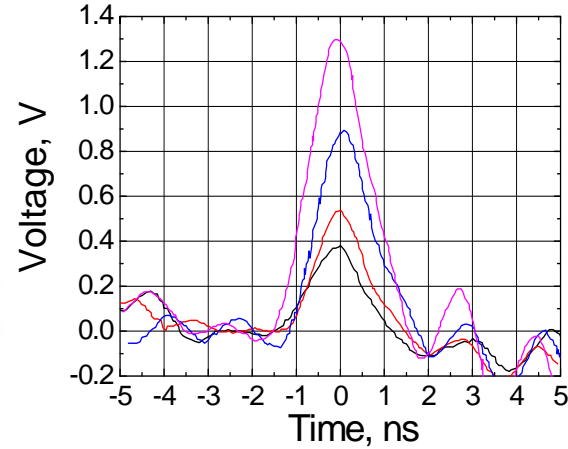


Fig. 4 SSPD photoresponse waveform transients taken with different light attenuation. Four different amplitudes are observed.

Figure 2(a). Figure 2(b) presents the simplified drawing, in which the arrows show the directions of the bias current flow. The first step of the PNR-SSPD fabrication is the e-beam patterning of the straight lines from which the NbN film will be removed to form the future meanders; these are grey in Figure 2(b). This step is the most important for the high quality SSPD fabrication and it is performed exactly in the same way as it was with the traditional SSPDs. The second step is the patterning of the parallel meander wiring shown as white stripes in Figures 2(a) and 2(b). Subsequently, the planar resistors are formed from 30-nm-thick gold film. Varying their length and width, as well as the thickness of the gold film we can vary their resistance. For the 5-section SSPD we used resistors of $0.5 \mu\text{m} \times 20 \mu\text{m}$ having the resistance of about 100Ω . Finally, the film around the meanders and their wiring is removed to form the completed PNR-SSPD device.

Thus, we have a device consisting of high quality meanders covering an area of $10 \mu\text{m} \times 10 \mu\text{m}$. Being patterned in the same way as the conventional single-meander SSPDs they are expected to have the same high quantum efficiency up to 30%.

Simultaneously, the division of one long meander into several short meanders reduces the SSPD recovery time. Indeed, after the disappearance of the hot spot the SSPD bias current recovers during the characteristic time $\tau = L_{\text{kin}}/R_{\text{series}}$, where L_{kin} is the kinetic inductance of the strip and R_{series} is the resistance connected in series with the SSPD. It is usually the equivalent resistance of the transmission line. For the traditional SSPD this time is approximately 10 ns and limits the counting rate to ~ 100 MHz. When the meander is divided into N sections connected in parallel the equivalent inductance of such a device is N^2 times smaller, and consequently the recovery time is also N^2 times smaller. For the 5-section SSPD it gives $\tau \approx 0.4$ ns, and for 10 sections it gives ~ 0.1 ns leading to GHz counting rates.

IV. EXPERIMENTAL SETUP, RESULTS, AND DISCUSSION

In the experimental setup the radiation of a pulsed semiconductor laser (operating at 0.85- μm wavelength with 20-ps pulse width and 100 kHz maximum repetition rate) was fed into a fiber with a variable fiber-based optical attenuator and then divided in two parts. One part was fed to the power meter whereas the other part after further fixed-value attenuation was fed to the fiber-coupled SSPD. The SSPD was immersed in liquid helium at 4.2 K temperature. The electrical photoresponse pulse was fed to a coaxial cable and then to amplifiers, a pulse counter, and an oscilloscope. The laser and the oscilloscope were triggered simultaneously by a pulse generator.

First, we measured the response time of the PNR-SSPD in a single-photon detection regime. It was significantly smaller than for traditional SSPD. Figure 3 presents the waveform transient acquired with the sampling oscilloscope and 0.01GHz to 2 GHz band, 45 dB gain low noise amplifiers. The full width at half maximum (FWHM) was 450 ps. For comparison, the traditional SSPD has FWHM of about 5.5 ns when measured in the same set up. Next, we varied the light attenuation and studied the probability of photoresponse and its magnitude depending on the attenuation. The main goal of this experiment was to prove that the observed effect is really the photon number resolution. We had to use amplifiers with 500 MHz band to have ~ 70 dB amplification required for our single-shot oscilloscope. Four different magnitudes were clearly observed for different light attenuations, as shown in Figure 4. The duration of the acquired waveform transients is significantly affected by the band of the amplifiers; actually, the response time is significantly smaller than presented in Figure 4. With the increase of the number of photons in the laser pulse incident on the PNR-SSPD the probability to observe higher response magnitude increases.

For a mean number of m photons per pulse, the probability $P(n)$ of detecting n photons from a given pulse is $P(n) \sim (e^{-m} m^n) / (n!)$. When $m \ll 1$ due to attenuation, the probability $P(n)$ simplifies to

$$P(n) \sim \frac{m^n}{n!}$$

Consequently, the probability of detecting one photon is proportional to m , the probability of detecting two photons is proportional to m^2 , and so on. Figure 5 presents relative detection

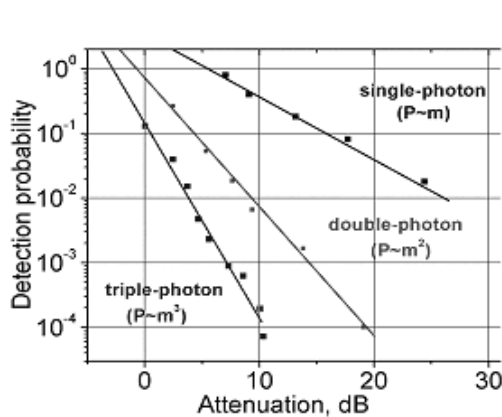


Fig. 5. Detection probability vs optical attenuation of laser pulse. Single-photon, double-photon and triple-photon regimes are clearly observed.

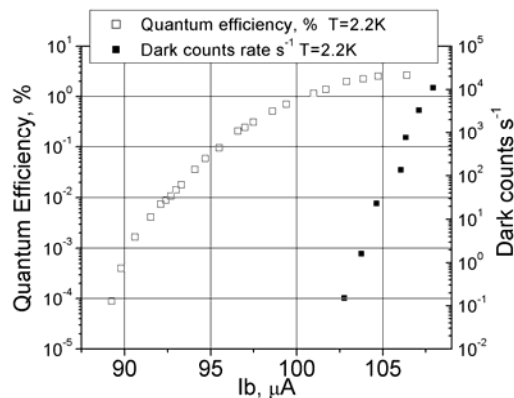


Fig. 6. Quantum efficiency at 1.3 μm wavelength (open symbols) and dark count rates (closed symbols) of PNR SSPD measured at 2.2K temperature.

probabilities versus optical attenuation of the laser pulse for the pulses of three different magnitudes.

The top curve corresponds to the pulses of smallest magnitude. The middle and the lowest curves in Figure 5 are taken for the pulses of higher magnitudes. In general, the analysis of the counter data is not straightforward as it requires taking into account the photoresponses for different number of photons. For example, when the counter threshold is set to two-photon detection events it counts also all other multi-photon events, as they have higher magnitude. But in the plot of Figure 5 the light intensities and the discriminator level we chose so that for a given point the contribution of other undesired multi-photon counts was significantly smaller. In this case, their contribution is smaller than the error of the measurement and does not play any significant role. Thus Figure 5 clearly demonstrates the capability of the detector to resolve one, two and three photons simultaneously absorbed.

Finally, we measured quantum efficiency η at 1.3 μm wavelength and dark counts rate R_{dk} of the PNR-SSPD. Figure 6 presents these results measured at 2.2 K temperature. One can see that the PNR-SSPD exhibits $\eta \approx 2.5\%$ and $R_{\text{dk}} \approx 0.1 \text{ s}^{-1}$. Quantum efficiency about an order of magnitude smaller than reported for the traditional SSPD can be attributed to the misalignment and coupling losses between the PNR-SSPD and the fiber.

V. CONCLUSION

We have demonstrated a novel design of the SSPD, which features both a photon-number-resolving (PNR) capability and a significantly reduced response time. The photoresponse pulses of four different distinct magnitudes were clearly observed. The detection probability *versus* mean number of photons in the laser pulse m was proportional to m^1 for single-photon detection events, to m^2 for double-photon events, and to m^3 for triple-photon events. This is the main proof of PNR-capability. The full width at half-maximum was as low as 450 ps allowing us to reach $\sim 1\text{GHz}$ counting rate. The PNR-SSPD exhibited $\sim 2.5\%$ quantum efficiency at 0.1 s^{-1} dark counts rate.

ACKNOWLEDGEMENT

Funding from the European Commission under project "SINPHONIA", contract number NMP4-CT-2005-16433, is acknowledged.

REFERENCES

- [1] Gol'tsman G. *et al*, *Appl. Phys. Lett.* **79**, 705 (2001).
- [2] Verevkin A. *et al*, *Appl. Phys. Lett.* **80**, 4687 (2002).
- [3] Semenov A. *et al*, *Physica C* **352**, 349 (2001).
- [4] Korneev A. *et al*, *Appl. Phys. Lett.* **84**, 5338 (2004).
- [5] Milostnaya I. *et al*, *Journal of Physics: Conference Series* **43**, 1334 (2006).
- [6] Rosfjord K. *et al*, *Optics Express* **14**, 527 (2006).
- [7] Gol'tsman G. *et al*, *IEEE Trans. on Appl. Supercond.* **17**, 246 (2007).
- [8] Verevkin A. *et al*, *Journal of Modern Optics* **51**, 1447 (2004).
- [9] Kerman A. *et al*, *Appl. Phys. Lett.* **88**, 111116 (2006).
- [10] Slysz W. *et al*, *Appl. Phys. Lett.* **88**, 261113 (2006).
- [11] Takesue H. *et al*, *Nature Photonics* **1**, 343 (2007).
- [12] Hadfield R. *et al*, *Appl. Phys. Lett.* **89**, 241129 (2006).
- [13] Rosenberg R. *et al*, *Appl. Phys. Lett.* **88**, 021108 (2006).
- [14] Robinson B. *et al*, *Optics Letters* **31**, 444 (2006).
- [15] Stevens M. *et al*, *Appl. Phys. Lett.* **89**, 031109 (2006).
- [16] Hadfield R. *et al*, *Optics Express*, **13**, 10846 (2005).